

ATMOSPHERIC ENVIRONMENT

Atmospheric Environment 36 (2002) 5741-5748

www.elsevier.com/locate/atmosenv

Short communication

Modeling surface-mediated renoxification of the atmosphere via reaction of gaseous nitric oxide with deposited nitric acid

Eladio M. Knipping, Donald Dabdub*

Department of Mechanical and Aerospace Engineering, University of California at Irvine, Irvine, CA 92697-3975, USA

Received 14 April 2002; accepted 3 August 2002

Abstract

Air quality models consider the formation and deposition of nitric acid (HNO₃) on surfaces to be an irreversible sink of atmospheric nitrogen oxides (NO_x) and therefore an effective termination step in the ozone formation cycle. However, experimental evidence suggests that the reaction of gaseous nitric oxide with nitric acid on surfaces may convert HNO₃ to photochemically active NO_x. A first-order simulation of this surface-mediated renoxification process is performed using an air quality model of the South Coast Air Basin of California. Peak ozone concentrations are predicted closer to observed values in regions regularly underpredicted by base case models. In certain regions, ozone predictions are enhanced by as much as ~ 30 ppb or $\sim 20\%$ compared to the baseline simulation. These results suggest that renoxification processes may be a key to resolving long-standing shortcomings of air quality models, in addition to reconciling [HNO₃]/[NO_x] ratios in remote regions. This study also illustrates that the surface terrain may play a more active chemical role than hitherto considered in air quality models. © 2002 Elsevier Science Ltd. All rights reserved.

Keywords: Renoxification; Surface reaction; Ozone; Deposition; Urban photochemical model

1. Introduction

Air quality models predict concentrations of ambient species through numerical solution of equations that mathematically describe physical and chemical processes in the atmosphere. The traditional role of the terrestrial surface in the evolution of atmospheric species in three-dimensional Eulerian chemical transport models is well defined. First, physical characteristics of the terrain affect the stability of the boundary layer and transport of species therein. Second, the terrain serves as a location for the emission of atmospheric species from anthropogenic and natural sources. Finally, the terrain provides surfaces for deposition of gases and deposition/settling of particles. Deposited species are lost irrever-

The mechanism leading to ozone formation in urban regions is well understood. Hydroxyl radicals (or other atmospheric oxidants) initiate the oxidation of organic compounds to form organic peroxy (RO₂) and hydroperoxy (HO₂) radicals. RO₂ and HO₂ radicals oxidize nitric oxide (NO) to nitrogen dioxide (NO₂). Nitrogen dioxide then photolyzes to form NO and ground-state oxygen atom, O(³P), which undergoes an association reaction with oxygen to form ozone. The photodissociation of ozone regenerates hydroxyl radicals propagating the reactions in a cycle. The formation of nitric acid (HNO₃) from the reaction of NO₂ and OH

$$NO_2 + OH \rightarrow HNO_3,$$
 (1)

is considered a dominant termination step in the ozone formation cycle through efficient surface deposition and/ or partitioning to the aerosol-phase (Meng et al., 1997). However, there is evidence that nitric acid deposited on

E-mail address: ddabdub@uci.edu (D. Dabdub).

1352-2310/02/\$ - see front matter © 2002 Elsevier Science Ltd. All rights reserved. PII: S 1 3 5 2 - 2 3 1 0 (0 2) 0 0 6 5 2 - 0

sibly to the ground and do not undergo any further reaction in the models.

^{*}Corresponding author. Tel.: +1-949-824-6126; fax: +1-949-824-8585

natural and anthropogenic surfaces could undergo further chemical processing.

Laboratory results from Finlayson-Pitts and coworkers (Mochida and Finlayson-Pitts, 2000; Saliba et al., 2000, 2001) show that gaseous nitric oxide reacts with nitric acid adsorbed on silica surfaces at relative humidities around 50%,

$$NO_{(g)} + HNO_{3(surface)} \rightarrow NO_2 + HONO,$$
 (2)

to form nitrogen dioxide and nitrous acid (HONO). The investigators detect small amounts of gas-phase HONO indicating that the fate of the nitrous acid product in the experimental system may be further reaction with adsorbed nitric acid or a surface-mediated self reaction,

$$HONO + HNO_{3(surface)} \rightarrow NO_2 + NO_2 + H_2O,$$
 (3)

$$HONO + HONO \rightarrow NO + NO_2 + H_2O.$$
 (4)

In brief, Reactions 2–4 could contribute to 'renoxification' of the atmosphere—the regeneration of nitrogen oxides ($NO_x = NO + NO_2$) from nitric acid.

The conversion of HNO₃ to NO_x has been suggested in previous studies in order to reconcile discrepancies between modeled and observed $[HNO_3]/[NO_x]$ ratios in the remote troposphere. Theories include the liquidphase reaction of HNO3 and formaldehyde in aerosol particles to generate formic acid and ultimately NO_x (Chatfield, 1994) and the reduction of HNO₃ to NO_x on soot particles (Hauglastine et al., 1996; Lary et al., 1997). However, recent investigations show that surface saturation occurs quickly on soot particles, i.e. the number of active surface sites responsible for the reduction of HNO3 are not regenerated after reaction (Kirchner et al., 2000; Disselkamp et al., 2000). The HNO₃-soot renoxification process is therefore rendered insignificant (Longfellow et al., 2000; Saathoff et al., 2001) leading to further study of alternative renoxification theories. Although such disparate [HNO₃]/[NO_x] ratios have not been reported in polluted urban areas amid high emissions of nitrogen oxides, it is reasonable to infer that renoxification processes may occur to a certain extent in urban regions as well. In this manuscript, we explore for the first time the influence of renoxification initiated by Reaction 2 to the ozone chemistry of an urban environment.

2. Model formulation

The CalTech Airshed Model is applied to the South Coast Air Basin of California simulating conditions present during the 1987 South Coast Air Quality Study (SCAQS) on 27–28 August 1987 (Meng et al., 1998). The model incorporates a size-resolved and chemically resolved dynamic aerosol module within a three-dimensional gas-phase model. Derivation of meteorological

fields, such as inversion base heights, and gas-phase emissions data are described by Harley et al. (1993). Gas-phase chemistry in the model is based on the LCC mechanism of Lurmann et al. (1987) with extensions by Harley et al. (1993). Derivation of particulate matter emissions data and treatment of secondary organic and inorganic aerosol formation are summarized by Meng et al. (1998).

In addition to Reaction 2, nitric acid can also be produced in the model via hydrogen atom abstraction from volatile organic compounds by nitrate radicals and via the gas-phase hydrolysis of dinitrogen pentoxide (N_2O_5). At the present moment, hydrolysis of N_2O_5 following uptake into the aqueous component of aerosol particles is not included in the CIT Airshed model.

The atmospheric diffusion equation,

$$\frac{\partial c_i}{\partial t} + \mathbf{u} \cdot \nabla c_i = \nabla \cdot (\mathbf{K} \cdot \nabla c_i) + R_i(\mathbf{c}, t, T) + E_i(\mathbf{x}, t) - S_i(\mathbf{x}, t)$$
(5)

describes the temporal and spatial evolution of gasphase species. In the above equation, c_i are the elements of the concentration vector \mathbf{c} , t is time, \mathbf{x} represents the spatial coordinates (x, y, z), \mathbf{u} represents the wind field components (u, v, w), \mathbf{K} is the eddy diffusivity tensor, R_i is the net chemical production or loss of species i, and T is temperature. E_i and S_i are the emission and removal fluxes of species i.

Dry deposition at the surface is a significant removal process of gas-phase species. The deposition flux is expressed in terms of a deposition velocity, $v_{\rm d}$. Seinfeld and Pandis (1998) present a detailed treatment of the determination of deposition velocities. In brief, the deposition velocity is considered via electrical analogy as the inverse of the sum of three resistances in series,

$$v_{\rm d} = \frac{1}{r_{\rm t}} = \frac{1}{r_{\rm a} + r_{\rm b} + r_{\rm c}},\tag{6}$$

where $r_{\rm t}$ is the total resistance. The first of the individual resistances, $r_{\rm a}$, represents the limitation due to turbulent transport down through the atmospheric surface layer, i.e. the aerodynamic resistance. After crossing the surface layer, gas-phase species encounter a thin quasi-laminar sublayer where transport to the surface is governed by molecular diffusion and denoted by $r_{\rm b}$, the quasi-laminar resistance. Finally, a canopy resistance, $r_{\rm c}$, represents the limitation due to uptake on the surface. Nitric acid is predicted by the CIT Airshed model to deposit on 65–80% of all surface contacts of nitric acid. For nitric oxide, deposition is much less effective with only 2–6% of surface contacts resulting in deposition.

By removing the canopy (uptake) resistance term from the expression for the deposition velocity, a contact velocity can be extracted, i.e.

$$v_{\text{contact}} = \frac{1}{r_{\text{a}} + r_{\text{b}}}. (7)$$

The contact velocity is dependent on parameters such as wind velocity, surface roughness and atmospheric stability.

Renoxification in the model is determined by evaluating two processes: the deposition rate of gas phase nitric acid and the surface contact rate of nitric oxide. The rate of Reaction 2, R_2 , is determined by selecting the rate-limiting of these two processes and dividing by the height of the first vertical layer, H_1 ,

$$R_2 = \min \{v_d[HNO_3], v_{contact}[NO]\}/H_1.$$
 (8)

The NO_2 and HONO products are released to the gas phase. Further surface reactions are not considered in the simulation. Fig. 1 illustrates the magnitude of the deposition rate for nitric acid and the surface contact rate for nitric oxide.

Finlayson-Pitts and coworkers performed experiments on silica surfaces only. Although silica surfaces are present on soils and building materials, a variety of natural (soil, mineral, plant) and anthropogenic (bituminous, metal, concrete and glass) surfaces are also present in urban environments. These surfaces, and coatings (paints and sealants), may influence the probability of Reaction 2. However, the rate of reaction appears to be dependent on the number of monolayers of surface-adsorbed water, with an optimal experimental

value reported as \sim 3 monolayers (Saliba et al., 2001). Other experiments show that typical urban surfaces hold approximately 3 water monolayers over a wide range of relative humidities (Lammel, 1999), thus supporting the transfer of the silica-surface experimental results to other materials.

The appropriateness of the model rate for Reaction 2 depends on a variety of factors. Indeed, a reaction probability of unity is chosen and limited solely as described earlier. The true reaction probability is expected to be much less. However, the representation within the model is conservative in several aspects. During intervals when the surface contact rate of NO becomes rate-limiting, accumulation of nitric acid on surfaces may occur. Particulate nitrate that has deposited or settled to the terrestrial surface may also provide added sites for Reaction 2 to occur. The aerosol surface area to air-parcel volume ratio $(S_{aerosol}/V_{air})$ in the model reaches values up to 0.06 m⁻¹, indicating that in some regions aerosol particles may provide as much surface area (albeit not entirely as nitric acid) as an idealized flat model terrain within 17 m of ground level and provide up to ~ 65 times the surface area of a flat terrain up to the top boundary of the model (1100 m). Aerosol nitrate mass is highly available in many regions of the model, as illustrated in Fig. 2 by plotting

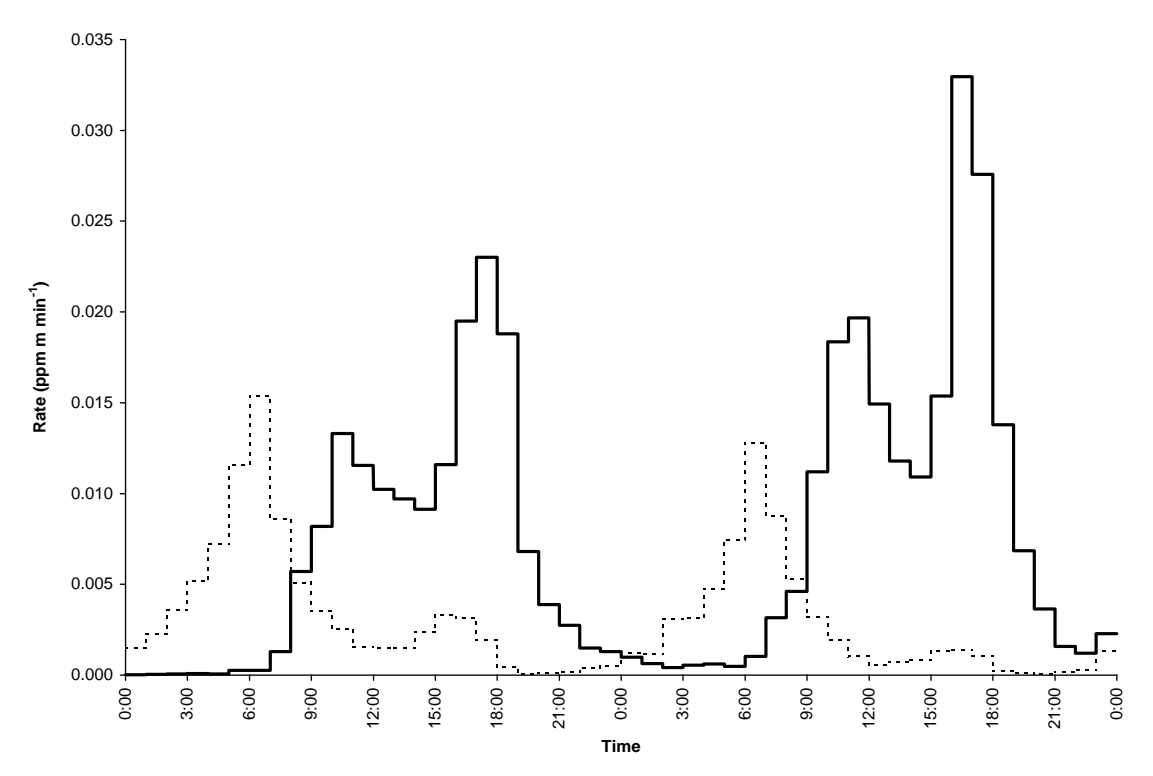


Fig. 1. Model predicted HNO₃ deposition and NO surface contact rates for Riverside for 27–28 August 1987; solid line: HNO₃ deposition rate, dashed line: NO surface contact rate.

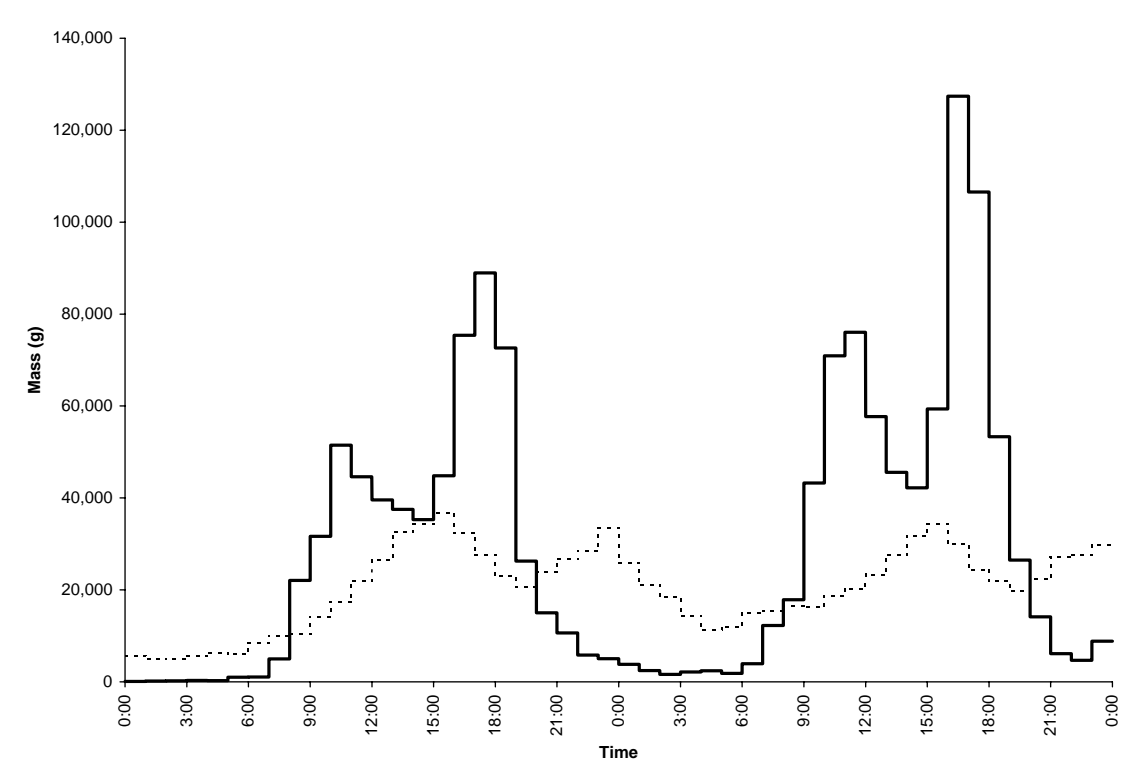


Fig. 2. Model predicted hourly HNO₃ deposited mass and 1-h average aerosol nitrate mass load for Riverside ($5 \text{ km} \times 5 \text{ km} \times 12.98 \text{ m}$ cell); solid line: deposited HNO₃, dashed line: aerosol nitrate load.

predicted hourly HNO₃ deposited mass and 1-h average aerosol nitrate mass loading at the lowermost computational cell containing the city of Riverside. (The cell has a height of 12.98 m and is 5 km \times 5 km wide.) Reaction 2 is not considered on aerosol particles due to the complexities of determining the extent of reaction on internally-mixed aerosol particles containing nitric acid, nitrate salts and other inorganic/organic components. However, reaction on aerosol particles is expected.

Other uncertainties also exist with respect to parameters within the CIT Airshed model, e.g. surface roughness and land use data. Notwithstanding the uncertainties, this simulation provides insight on the effect of potentially several renoxification processes on urban ozone chemistry. Sensitivity studies are performed to gauge the extent of renoxification necessary to affect ozone concentrations in the Southern California Air Basin.

3. Results and discussion

Fig. 3 shows the effect of the renoxification on ozone concentrations compared to a base case model simulation. Measured ozone concentrations are also shown. In general, second-day data are preferred for model

evaluations since these values are less affected by any artifacts introduced via initial conditions and better represent the chemical mechanism (or emission scenario) being evaluated.

Fig. 3 illustrates that inclusion of the renoxification mechanism increases second-day ozone peaks to values more consistent with ambient measurements than in the base case simulation. Two potential routes accountable for the increased ozone exist. First, the ozone formation cycle may be intensified due to conversion of NO to NO₂ at the surface. The NO₂ produced in the reaction may photolyze to form ozone directly (the sole reaction responsible for tropospheric ozone generation). Second, the nitrous acid product undergoes photodissociation to NO and OH and thus propagates the NO_x–VOC ozone cycle.

Predicted NO_x concentrations of the renoxification simulation are similar to those of the base case simulations. The mean ratio of predicted renoxification $[NO_x]$ versus $[NO_x]$ calculated by the base case simulation is $97\% \pm 6\%$ (1σ). However, Fig. 4 shows that HONO concentrations are elevated in the renoxification simulation by an order of magnitude above values predicted in the base case simulation. From these observations, it can be inferred that the increased ozone predictions are a result of elevated HONO levels. The

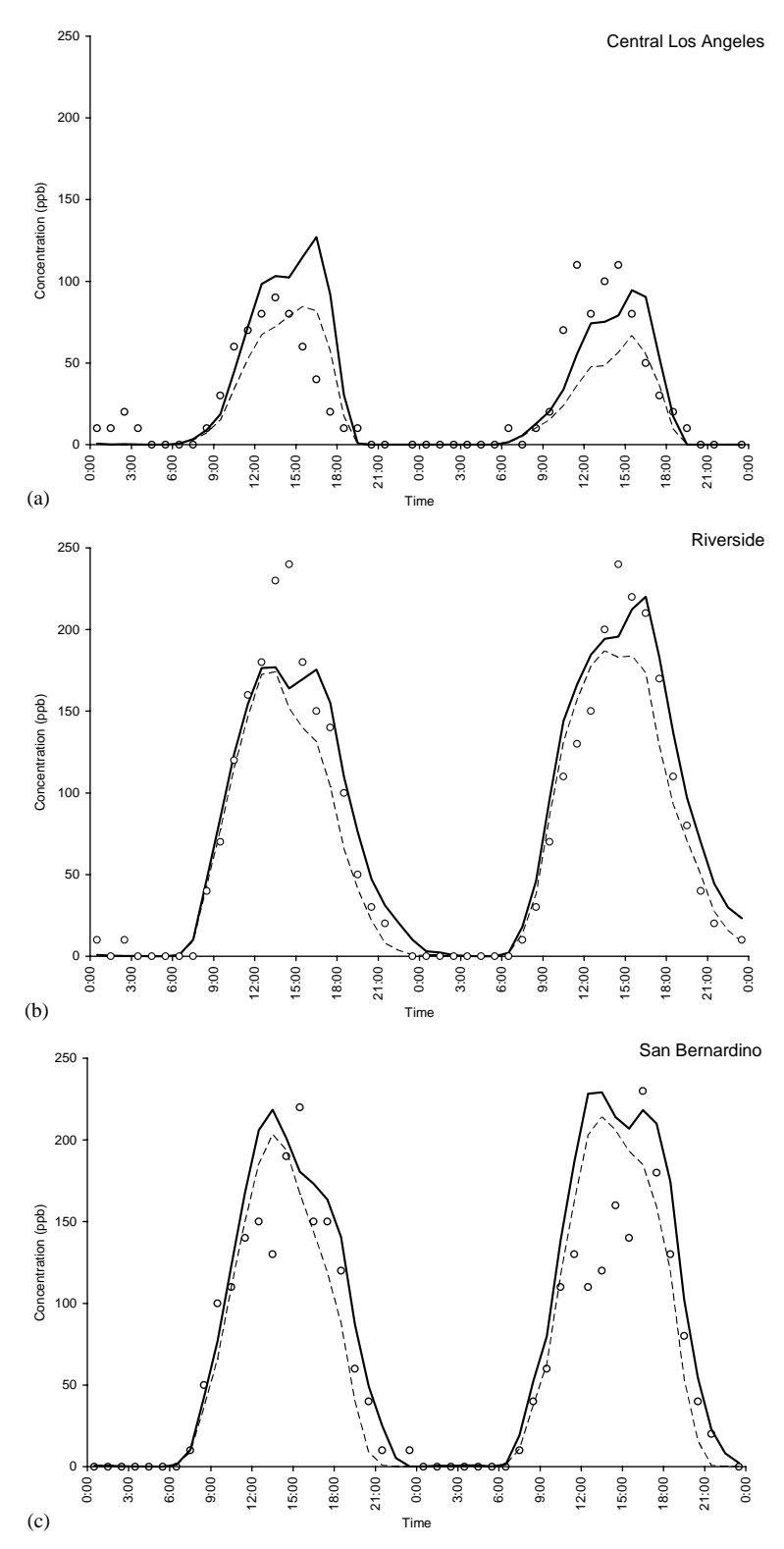


Fig. 3. Ozone concentration time series for 27–28 August 1987 for (a) Central Los Angeles (b) Riverside and (c) San Bernardino; solid line: renoxification, dashed line: base case, open circles: measurements.

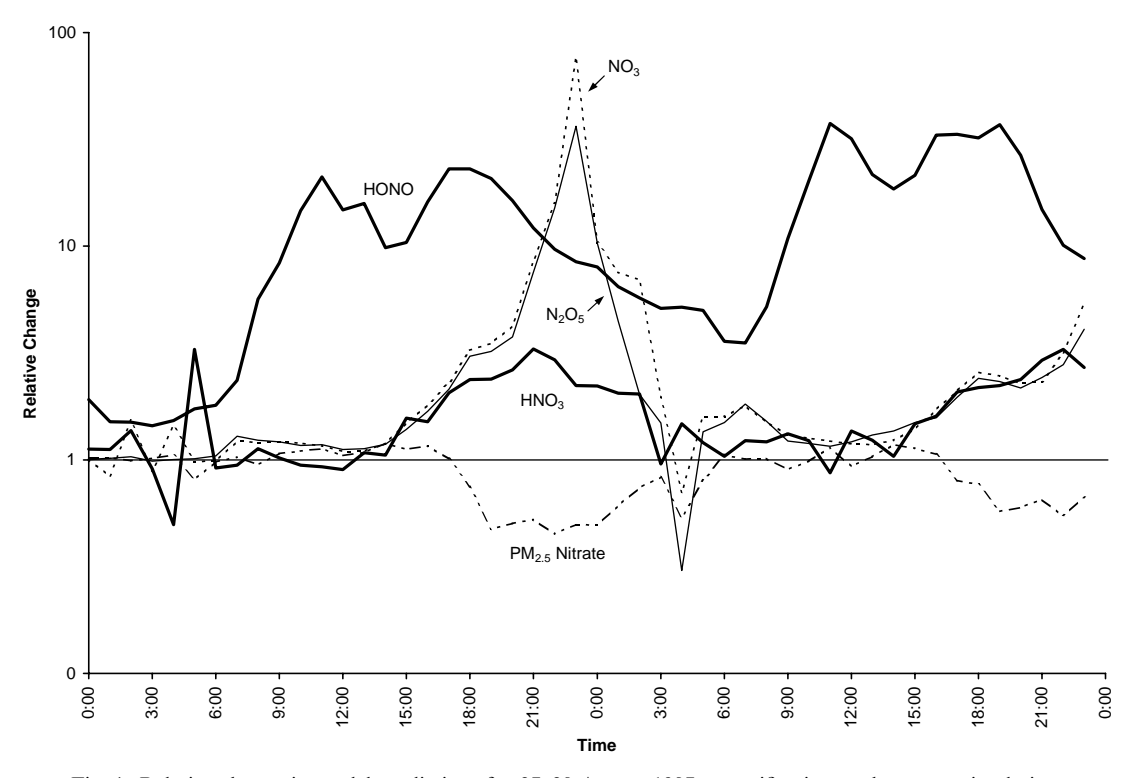


Fig. 4. Relative change in model predictions for 27-28 August 1987: renoxification vs. base case simulation.

Table 1 Comparison of predicted and observed peak ozone concentrations for 28 August 1987

	Peak ozone observed measurements ppb	Peak ozone base case simulation		Peak ozone renoxification simulation		Improvement base case vs. renoxification	
		ppb	Model vs. obs.	ppb	Model vs. obs.	ppb	%
Central LA	110	67	61%	95	86%	28	25%
Riverside	240	187	78%	220	92%	33	14%
San Bernardino	230	214	93%	229	~100%	15	7%

relative changes of other nitrogen species are also shown in Fig. 4. Lastly, total PM_{10} nitrate also showed little variance between the simulations, with a mean ratio of 105% + 8% (1σ).

Table 1 shows that addition of Reaction 2 increases predicted peak ozone concentrations by as much as 33 ppb in Riverside. Overall, peak ozone concentrations are predicted closer to observed values. In particular, the ozone peak in Central Los Angeles, a region where the photochemical models regularly underpredict ozone concentrations, is increased from 61% to 86% of observed values—an improvement of 25%. No other chemical process has been able to reconcile differences in ozone predictions in this area. Obtaining greater fidelity between observed 1-h peak O₃ values and predicted

concentrations in 25 km² computational cells is an important task in air quality models, as both the National Ambient Air Quality Standards and California Ambient Air Quality Standards are based on 1-h peak ozone concentrations.

In addition to peak fidelity, other statistical comparison between the renoxification and base case simulation is provided in Table 2. The period between 9:00 a.m. and 9:00 p.m. on 28 August, 1987, is used to calculate a 12-h mean ozone concentration, standard deviation and the root-mean-square, *RMS*, of the model predictions. (During this time period ozone concentrations are above background values and are not lowered due to nighttime titration by nitrogen oxides.) The root-mean-square is obtained as the square root of the mean squared

59

Observed data Renoxification simulation Base case simulation Std. dev. Mean Mean Std. dev. **RMS** Mean Std. dev. RMS Central LA 58 19 34 22 35 51 19 26 Riverside 143 54 134 51 30 156 54 27

63

48

Table 2 12-h (9:00 a.m. - 9:00 p.m.) statistical data of predicted and observed O_3 values for 28 August 1987^a

143

San Bernardino

deviation of predicted values from observed data, i.e.

64

124

$$RMS = \sqrt{\frac{1}{N} \sum_{i=1}^{N} (c_{i,\text{pred}} - c_{i,\text{obs}})^2},$$
 (9)

where N is the number of data points analyzed. All statistical measurements of the renoxification simulation shown in Tables 1 and 2 are either as reliable or show a marked improvement when compared to the base case simulation except for the 12-h mean and RMS ozone values at San Bernardino. This late-morning and early-afternoon dampening of ozone concentrations recalls that uncertainties may also exist in measured data, as these can be influenced by localized events or have inherent defects. However, both models are unable to replicate this intriguing feature observed during the SCAOS episode in San Bernardino.

Another important feature of the renoxification simulations is the prediction of double ozone peaks at the Riverside and San Bernardino sites. Although the observed values do not show clearly a presence of a double peak, these double peaks have been a common occurrence in the downwind regions of the South Coast Air Basin of California. Once more, no other chemical process has been able to reproduce such effects in air quality models.

Notwithstanding the uncertainties in the treatment of Reaction 2, sensitivity runs were performed by lowering the probability of Reaction 2 by successive orders of magnitude. At a reaction probability of 0.1, ozone concentrations were found to be typically within 2% of the predictions of the base case simulation. Further studies should be performed in order to determine the appropriateness of the modeling approach used in this first-order study. In addition, other renoxification processes should be explored, particularly in aerosol particles, since inclusion of renoxification processes appears to resolve some lasting, important shortcomings of air quality models.

4. Conclusion

A first-order simulation of a surface-mediated renoxification process has been performed. Inclusion of the reaction of gaseous nitric oxide with deposited nitric acid into an air quality model of the South Coast Air Basin of California indicates that renoxification processes may resolve long-standing deficiencies of air quality models. The shortcomings include the accurate prediction of ozone concentration peaks in the Los Angeles area and the prediction of double-peaks in downwind areas of the basin.

64

170

Undoubtedly, there are several uncertainties that must be addressed before the renoxification process explored in this paper can be quantified accurately by atmospheric models. However, results suggest that inclusion of some renoxification processes may be an important mechanism in reconciling ozone predictions with observations in urban regions, in addition to reconciling $[HNO_3]/[NO_x]$ ratios in remote regions. Finally, this study also illustrates that the surface terrain may play a more active chemical role than hitherto considered in air quality models.

Acknowledgements

This work was funded by the Link Foundation's Energy Fellowship Program and National Science Foundation CAREER Award Grant No. ATM-9985025. Any opinions, findings, and conclusions or recommendations expressed in this material are those of the authors and do not necessarily reflect the views of the National Science Foundation. The authors thank Professor Barbara Finlayson-Pitts for helpful discussions and comments on the manuscript.

References

Chatfield, R.B., 1994. Anomalous HNO₃/NO_x ratio of remote tropospheric air: Conversion of nitric acid to formic acid and NO_x? Geophysical Research Letters 21, 2705–2708.

Disselkamp, R.S., Carpenter, M.A., Cowin, J.P., 2000. A chamber investigation of nitric acid-soot aerosol chemistry at 298 K. Journal of Atmospheric Chemistry 37, 113–123.

Harley, R.A., Russell, A.F., McRae, G.J., Seinfeld, J.H., 1993. Photochemical modeling of the Southern California Air Quality Study. Environmental Science and Technology 27, 378–388.

^a All values have units of ppb.

- Hauglastine, D.A., Ridley, B.A., Solomon, S., Hess, P.G., Madronich, S., 1996. HNO₃/NO_x ratio in the remote troposphere during MLOPEX 2: evidence for nitric acid reduction on carbonaceous aerosols? Geophysical Research Letters 23, 2609–2612.
- Kirchner, U., Scheer, V., Vogt, R., 2000. FTIR spectroscopic investigation of the mechanism and kinetics of the heterogeneous reaction of NO₂ and HNO₃ with soot. Journal of Physical Chemistry 104, 8908–8915.
- Lammel, G., 1999. Formation of nitrous acid: parameterisation and comparison with observations. Max-Planck-Institut Für Meteorologie, Hamburg, Report No. 286.
- Lary, D.J., Lee, A.M., Toumi, R., Newchurch, M.J., Pirre, M., Renard, J.B., 1997. Carbon aerosols and atmospheric photochemistry. Journal of Geophysical Research 102, 3671–3682.
- Longfellow, C.A., Ravishankara, A.R., Hanson, D.R., 2000. Reactive and nonreactive uptake on hydrocarbon soot: HNO₃, O₃ and N₂O₅. Journal of Geophysical Research 105, 24345–24350.
- Lurmann, F.W., Carter, W.P.L., Coyner, L.A., 1987. A surrogate species chemical reaction mechanism for urbanscale air quality simulation models, Vols. I and II. Report to the U.S. Environmental Protection Agency, Contract 68-02-4104, ERT Inc., Newbury Park, California, and Statewide Air Pollution Research Center, University of California, Riverside.

- Meng, Z., Dabdub, D., Seinfeld, J.H., 1997. Chemical coupling between atmospheric ozone and particulate matter. Science 277, 116–119.
- Meng, Z., Dabdub, D., Seinfeld, J.H., 1998. Size-resolved and chemically resolved model or aerosol dynamics. Journal of Geophysical Research—Atmospheres 103, 3419–3435.
- Mochida, M., Finlayson-Pitts, B.J., 2000. FTIR studies of the reaction of gaseous NO with HNO₃ on porous glass: Implications for conversion of HNO₃ to photochemically active NO_x in the atmosphere. Journal of Physical Chemistry A 104, 9705–9711.
- Saathoff, H., Naumann, K.-H., Riemer, N., Kamm, S., Mohler, O., Schurath, U., Vogel, H., Vogel, B., 2001. The loss of NO₂, HNO₃, NO₃/N₂O₅, and HO₂/HOONO₂ on soot aerosol: A chamber and modeling study. Geophysical Research Letters 28, 1957–1960.
- Saliba, N.A., Mochida, M., Finlayson-Pitts, B.J., 2000. Laboratory studies of sources of HONO in polluted atmospheres. Geophysical Research Letters 27, 3229–3232.
- Saliba, N.A., Yang, H., Finlayson-Pitts, B.J., 2001. Reaction of gaseous nitric oxide with nitric acid on silica surfaces in the presence of water at room temperature. Journal of Physical Chemistry A 105, 10339–10346.
- Seinfeld, J.H., Pandis, S.N., 1998. Atmospheric Chemistry and Physics: from Air Pollution to Climate Change. Wiley, New York, NY.